



Mechanisms of thermal shock failure for ultra-high temperature ceramic

Songhe Meng^a, Guoqian Liu^{a,*}, Yue Guo^a, Xianghong Xu^b, Fan Song^b

^aCenter for Composite Materials, Harbin Institute of Technology, Harbin 150080, China

^bState Key Laboratory of Nonlinear Mechanics, Institute of Mechanics, Chinese Academy of Sciences, Beijing 100190, China

ARTICLE INFO

Article history:

Received 30 June 2008

Accepted 21 August 2008

Available online 30 August 2008

Keywords:

Ceramic matrix

Sintering

Microstructure

Failure analysis

ABSTRACT

The materials considered in our analysis were ZrB₂ ceramic matrix composites. Effect of two different additives (graphite and AlN) on thermal shock stability for the materials was measured by water quench test. It showed that it may provide more stable thermal shock properties with additives of graphite. It was explained by different thermal properties and crack resistance of the two materials in detail. Surface oxidation was one of main reasons for strength degradation of ceramic with additives of graphite after quenched in water, and surface crack was one of main reasons for strength degradation of ceramic with additives of AlN after quenched in water.

It was presented that it was a potential method for improving thermal shock stability of ZrB₂ ceramic matrix composites by introducing proper quantities of graphite.

© 2008 Elsevier Ltd. All rights reserved.

1. Introduction

Zirconium diboride (ZrB₂) has many intrinsic characteristics, such as high melting point, high hardness, good chemical inertness, and high wear stability, which make it a promising candidate for high temperature structural materials [1–5]. However, it is too low for thermal shock stability of monotonic ZrB₂, which limit its application in re-entry space vehicles. Therefore, it is necessary to improve thermal shock stability of ZrB₂. It is a common way to improve thermal shock behavior by improving its mechanical properties. Silicon carbide (SiC) particulate is a common reinforcement for ceramic materials due to its performances of high strength, high elastic modulus with good thermal stability.

Many researchers [6–10] have investigated thermal shock behaviors of ceramic matrix composites in both theories and experiments for many years. However, few investigations performed on thermal shock property of ultra-high temperature ceramic composites, such as large size ZrB₂ ceramic matrix composites.

In this work two kinds of materials were fabricated by hot-pressing: ZrB₂–20%SiC_p–10%graphite (ZSC) and ZrB₂–20%SiC_p–5%AlN (ZSA). The relative densities of the two materials were 92.74% and 96.9% for large size ZSC and ZSA, respectively, which were lower than that of small size ones (more than 99% relative density can be obtained). The processing method was reported. The mechanical properties and thermal shock behavior of ZrB₂ ceramic matrix composites for large size ones were studied.

2. Experimental procedures and theory

2.1. Material fabrication and test method

The powder mixtures ZSC was ball-milled for 14 h in a polyethylene bottle using ZrO₂ balls and ethanol as grinding media, and the same procedures for ZSA mixtures. After mixing, the slurry was dried in a rotary evaporator and screened. The resulting powder mixtures were hot-pressed at 1900 °C for 1 h under a uniaxial load of 30 MPa in Ar atmosphere. Two kinds of materials with a same size (ϕ 80 mm × 65 mm) were fabricated.

Mechanical properties of the two materials were measured using Instron 5848 Micro-Tester. Specimens were cut by linear cutting machine. Residual flexural strength was tested in three-point flexural test on 3 mm × 4 mm × 36 mm bars, using 30 mm span and a crosshead speed of 0.5 mm min⁻¹. Thermal conductivity and coefficients of thermal expansion were measured by Flash line 5000.

2.2. Characterization for resistance curve [11–13]

According to theory of indentation fracture, stress intensity factor of crack tip for indentation crack K as

$$K = K_{\sigma} + K_{\tau} \quad (1)$$

Applied stress by bending and residual stress by indentation, contributing to stress intensity factor, are as following:

$$\begin{aligned} K_{\sigma} &= \psi \sigma c^{1/2} \\ K_{\tau} &= \chi P c^{-3/2} \end{aligned} \quad (2)$$

* Corresponding author. Tel.: +86 451 86402432.

E-mail address: lgq_lxm@yahoo.com.cn (G. Liu).

Therefore, total stress intensity factor around crack tip of indentation is

$$K = K_{\sigma} + K_r = \psi\sigma c^{1/2} + \chi P c^{-3/2} \quad (3)$$

For a given indentation load P , failures occurred at that applied stress $\sigma = \sigma_{failure}$ which satisfied the “tangency condition”, as shown in the following equation:

$$\frac{dK'}{dc} = \frac{dK_{IC}}{dc} \quad (4)$$

Specimens were ground by fine abrasive papers. Vickers indentation method was used at 3, 5, 10, 20, 30, 50 kg force separately. Specimens with indentations were tested in three-point bending test, and pairs of (P, σ_r) were obtained. Crack resistance of the materials was obtained using method of envelope line.

2.3. Quench test

Thermal shock test equipment was electric muffle furnace. Water was kept constant to be 100 °C for use as quench medium. Temperature of heating and cooling systems of the thermal shock test apparatus for this experiment could be controlled within the limit of ±5 °C. In each thermal shock test, a specimen was heated for 10 min in the furnace and cooled for 5 min in the cooling bath to assure temperature uniformity. After quenched, specimens were dried and their residual strength values were measured using three-point flexural fixture with a span of 30 mm and a crosshead speed of 0.5 mm min⁻¹ with the temperature interval of 100 °C. Surface of specimens was observed by SEM.

3. Results and discussion

3.1 Results of thermal properties test

Coefficient of expansion and conductivity are two important factors for thermal shock properties. Thermal properties were tested on Flash line 5000 for two materials with different additives (shown by Fig. 1). As shown by Fig. 1, it is higher for conductivity of ZSC than that of ZSA among most of temperatures, which indicates a lower temperature gradient for ZSC. By contraries, coefficients of ZSC are lower than that of ZSA, which indicates lower thermal stress than that of ZSA at the same temperature gradient. As a result of thermal properties above, thermal shock property of ZSC should be higher than that of ZSA.

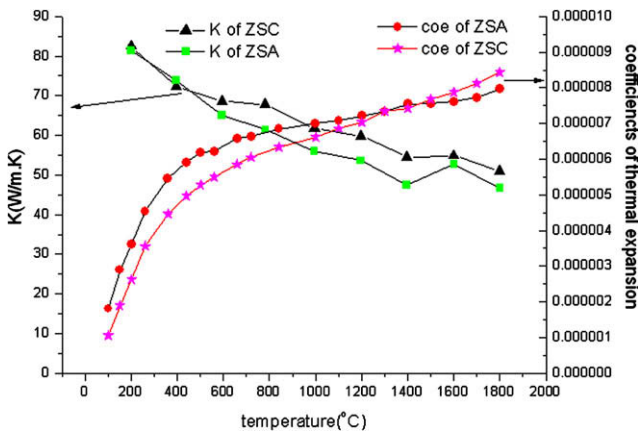


Fig. 1. Results of thermal properties of ZSC and ZSA.

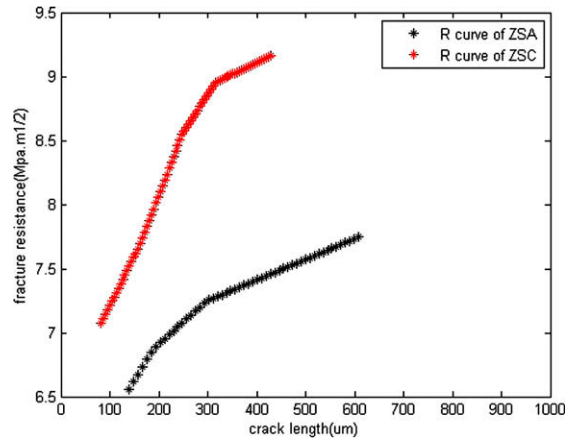


Fig. 2. Crack resistance of ZSA and ZSC.

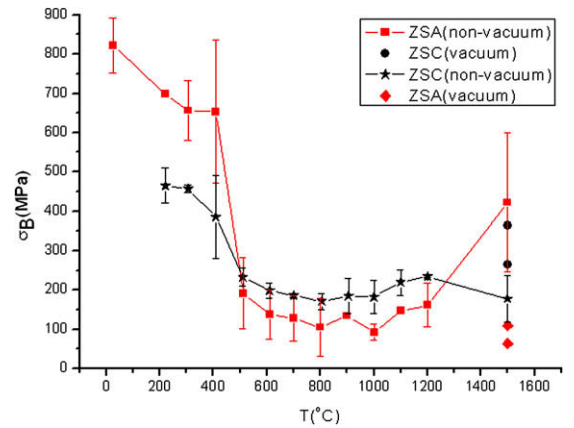


Fig. 3. Residual flexural strength dependent on quenching temperature.

3.2. Results of resistance curve

Resistance curves for the two materials are shown in Fig. 2. As can be seen, it is much higher for crack resistance of ZSC than that of ZSA, which can be confirmed by SEM that smaller indentation crack of ZSC appeared. As a result of mechanical properties above, thermal shock property should also be higher than that of ZSA.

3.3. Results of quench test

It is shown in Fig. 3 for residual strengths of the two materials. As shown, critical quench temperature is the same 400 °C for the two materials. Before quenching, strength of ZSA is higher than that of ZSC. At quench temperature of 400 °C, strengths are degraded at different degree for the two materials. After 400 °C, residual strength is retained for the two materials. Much more strength is lost for ZSA. Only 22.5% strength is retained for ZSA, and 44.4% for ZSC. Residual strength of ZSC is higher than that of ZSA. As can be seen from SEM, no distinct thermal shock crack appears on the surface of ZSA (Fig. 4a and b) before 400 °C, and distinct thermal shock cracks appear (Fig. 4c and d) after 400 °C. Among whole quenching temperatures, no distinct thermal shock cracks appear on the surface of ZSC (Fig. 4e and f). It is contributed by graphite for the higher crack resistance of ZSC, as thermal stress of the material was released for some extent by graphite due to its softness.

All above indicate that thermal shock stability of ZSC is much higher than that of ZSA, which is consistent with the result of thermal properties and resistance curve.

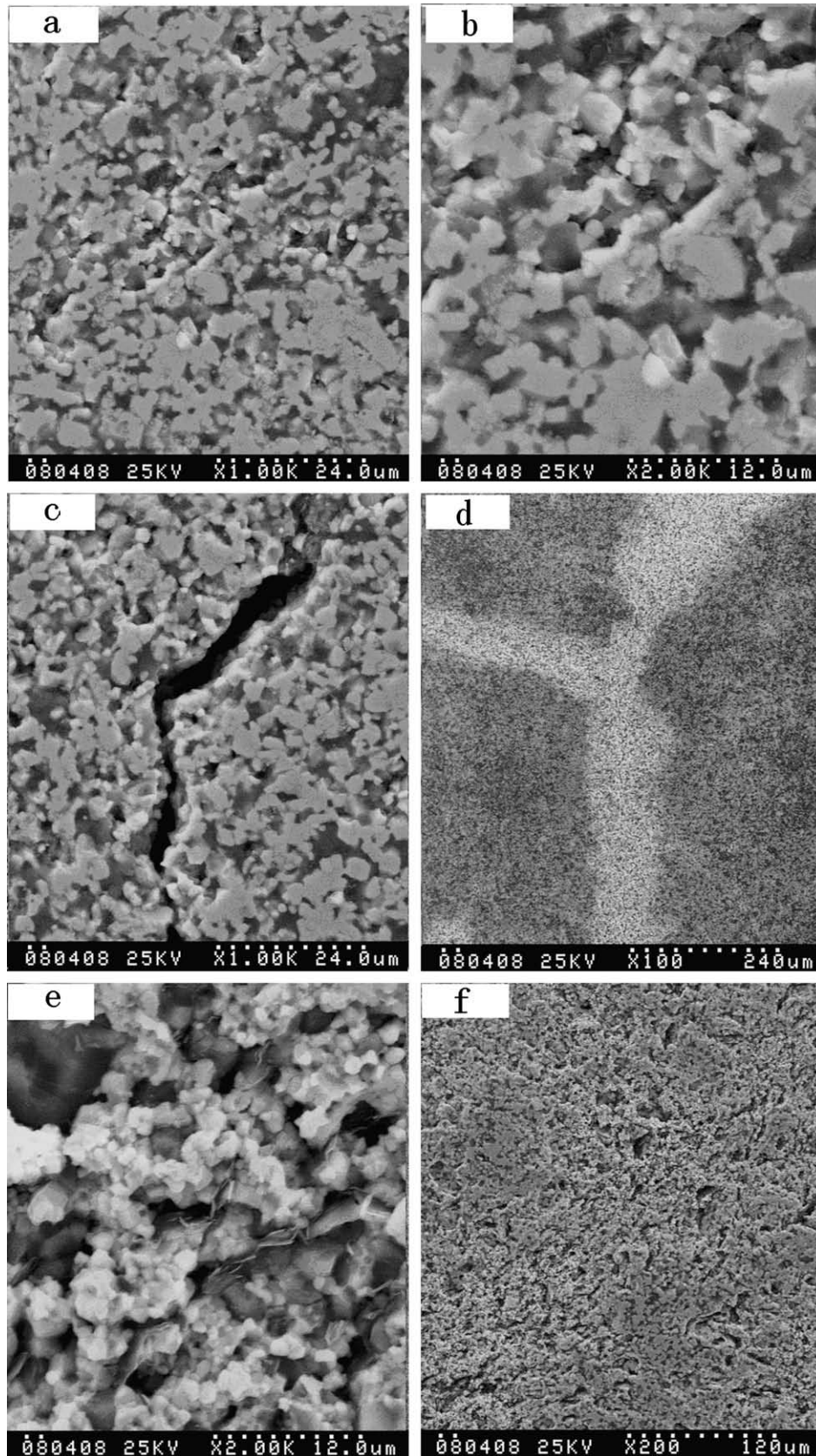


Fig. 4. (a,b) Surface pattern for ZSA after quenched from 300 °C; (c) surface pattern for ZSA after quenched from 500 °C; (d) surface pattern for ZSA after quenched from 1200 °C and (e,f) surface pattern for ZSC after quenched from 1200 °C.

As shown in Fig. 3, residual strength of ZSA ascends after quenching temperature of 1200 °C. As can be seen from SEM

(Fig. 5), it is attributed to surface crack healing by glass phase as a result of oxidation. However, as a result of B_2O_3 escaping from

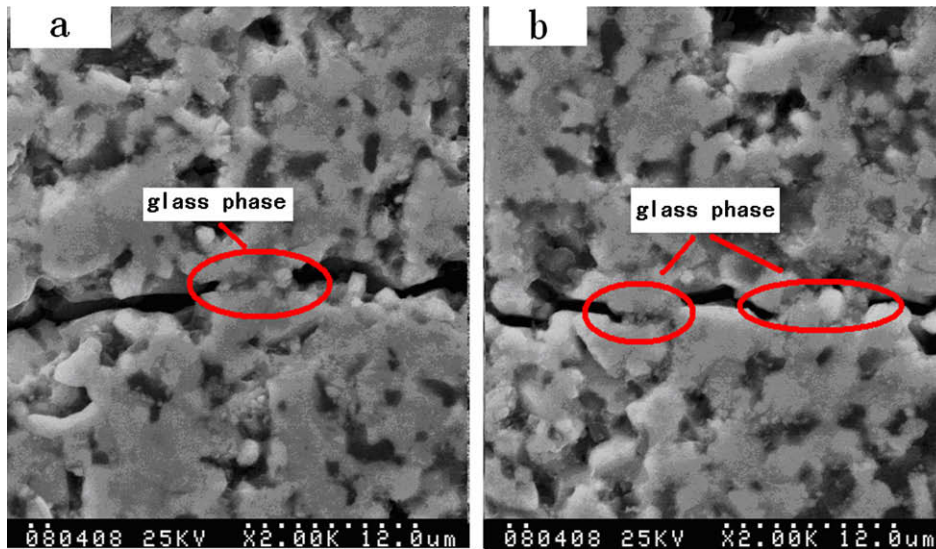


Fig. 5. Surface crack pattern (after ground) for ZSA after quenched from 1500 °C.

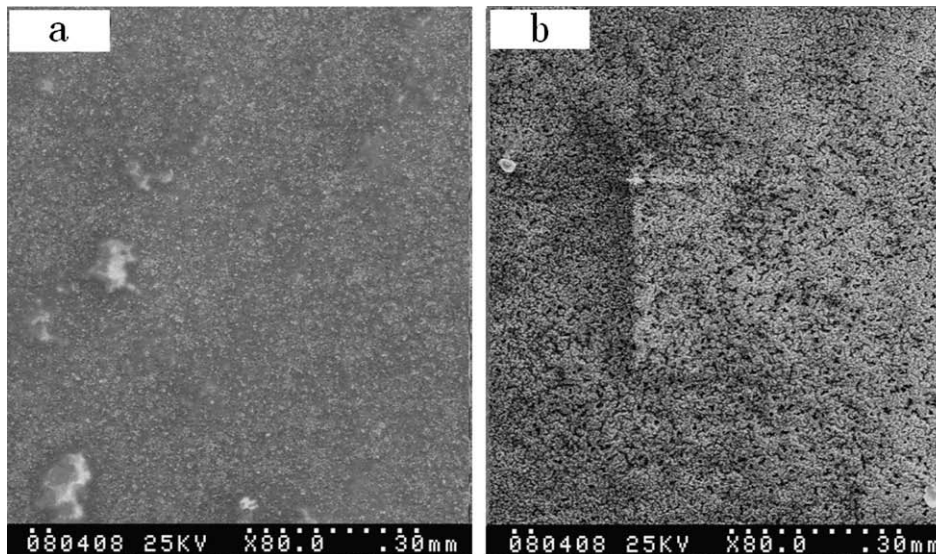


Fig. 6. (a) Surface pattern (before ground) for ZSA after quenched from 1200 °C and (b) surface pattern (before ground) for ZSA after quenched from 1500 °C.

surface, lots of voids were left on the surface of material (Fig. 6b), so residual strength at quenching temperature of 1500 °C scattered in a larger scale. Comparing residual strength of specimens quenched in atmosphere with that of specimens quenched in vacuum, it confirmed existence of crack healing mechanism as residual strength of specimens quenched in vacuum being lower than that of specimens quenched in atmosphere at the quenching temperature of 1500 °C.

In quenching test, it caused degradation of the two materials by surface oxidation, thermal shock cracks and thermal shock damage. As surface cracks clearly observed by SEM, it was the main reason for degradation of residual strength of ZSA after quenching tests. However, no surface cracks were observed after quenching test for ZSC. It was implicated that the main reasons for degradation of ZSC may be thermal shock damage and surface oxidation. As shown in Fig. 3, it is different between the trends of residual strength of ZSC quenched in vacuum and in non-vacuum. As shown, it is relatively higher for the residual strength of ZSC quenched in vacuum than that of ZSC quenched in non-vacuum. It proves that residual strength was affected by surface oxidation.

Therefore, surface oxidation was one of important factors for strength degradation of ZSC. It also showed that, it was relatively lower for residual strength of ZSC quenched in vacuum at 1500 °C than that of ZSC non-quenched in water. It proves that it was not a unique degradation mechanism of residual strength of ZSC for surface oxidation, and that thermal shock damage existed. Therefore, it can be improved by improving oxidation resistance for thermal shock stability of ZSC.

4. Conclusions

Thermal shock stability of the ceramic materials was characterized by water quench test. It shows that, different mechanisms of strength degradation exist for the two materials after quenched in water: surface crack is one of main reasons for strength degradation of ZSA, and residual strength ascends at quenching temperature of 1500 °C as surface cracks healed up by glass phase; Surface oxidation is one of important reasons for strength degradation of ZSC, and thermal shock damage is another important reason.

In conclusion, thermal shock stability of ZSC is better than that of ZSA. It is one of important methods to improve thermal shock stability by improving oxidation resistance for ZSC.

Acknowledgements

The authors are grateful for the support by National Science Foundation of China under grants #90505015.

References

- [1] Levine Stanley R, Opila Elizabeth J, Hallarge Michael C, Kiser James D, Singh Mrityunjay, Salem Jonathan A. *J Eur Ceram Soc* 2002;22:2757.
- [2] Monteverde Frédéric, Savino Raffaele. *J Eur Ceram Soc* 2007;27:4797.
- [3] Chamberlain AL, Fahrenheitz WG, Hilmas GE, Ellerby DT. *J Am Ceram Soc* 2004;87:1170.
- [4] Zheng Guo-jun, Zhen-Yan D, Naoki K, Jian-Feng Y, Tatsuki O. *J Am Ceram Soc* 2000;83:2330–2.
- [5] Zhang XingHong, Hu Ping, Han JieCai, Xu Lin, Meng SongHe. *Scripta Mater* 2007;57:1036.
- [6] Yang Zhi-Hua, Jia De-Chang, Zhou Yu, Meng Qing-Chang, Shi Peng-Yuan, Song Cheng-Bin. *Mater Chem Phys* 2008;107:476–9.
- [7] Kalantar M, Fantozzi G. *Mater Sci Eng: A* 2008;472:273–80.
- [8] Shen Liya, Liu Mingjian, Liu Xiaozhen, Li Bo. *Mater Res Bull* 2007;42:2048–56.
- [9] Sands CM, Henderson RJ, Chandler HW. *Comput Mater Sci* 2007;39:862–70.
- [10] Lee Joong Hyun, Park Sung Eun, Lee Hyung Jik, Lee Hong Lim. *Mater Lett* 2002;56:1022–9.
- [11] Cook RF, Liniger EG, Steinbrech RW, et al. Sigmoidal indentation-strength characteristics of polycrystalline alumina. *J Eur Ceram Soc* 1994;77(2):3059–62.
- [12] Gilbert CJ, Cao JJ, De Jonghe LC. Crack-growth resistance curve behavior in silicon carbide: small versus long cracks. *J Eur Ceram Soc* 1997;80(9):2253–61.
- [13] Lawn BR, Padture NP, Brawn LM, et al. Model for toughness curves in two-phase ceramics: I. Basic fracture mechanics. *J Eur Ceram Soc* 1993;76(9):2235–40.